Research Article

Determination of Optimum Conditions for the Production of Activated Carbon Derived from Separate Varieties of Coconut Shells

E. S. Sanni,[1] M. E. Emetere,[2] J. O. Odigure,[3] V. E. Efeovbokhan,[1] O. Agboola,[1] and E. R. Sadiku[4]

[1]*Department of Chemical Engineering, Covenant University, PMB 1023, Ogun State, Nigeria*
[2]*Department of Physics, Covenant University, PMB 1023, Ogun State, Nigeria*
[3]*Department of Chemical Engineering, Federal University of Technology, PMB 65, Niger State, Nigeria*
[4]*Department of Chemical, Metallurgical and Materials Engineering, Tshwane University of Technology, Pretoria, South Africa*

Correspondence should be addressed to E. S. Sanni; adexz3000@yahoo.com

Activated carbons were produced from coconut shells of tall and dwarf tree varieties. The activated carbon from the tall tree variety was initially synthesized using 1 M concentration of each of $ZnCl_2$, H_3PO_4, and KOH solutions. From the adsorptive tests conducted using methylene blue solution, the activated carbon produced with H_3PO_4 gave the best absorbance and adsorptive performance. Coconut shells of dwarf tree variety were then obtained and treated with same mass of coconut shells of the tall tree variety using varied concentrations of the acid in order to determine whether the optimum concentration and temperature for producing carbon black from the coconut shells are distinct or similar for both varieties. The process was also modelled using the Differential Response Method (DRM) in order to determine the yields and adsorptive performances of the activated carbons by varying the carbonization temperature and concentration. The results from experiment and the developed mathematical model were both found to be in agreement giving the optimum concentration of phosphoric acid and pH for producing activated carbon to be 0.67 M and 2.07 for the tall tree variety and 1 M and 1.98 for the dwarf variety at optimum temperatures in the range of 450–575°C and 575°C, respectively.

1. Introduction

Activated carbon, a carbonaceous material with characteristic surface area and highly developed porous structure, consists of 87 to 97% carbon with other trace elements [1]. It can be produced from coal, wood, agricultural, and paper wastes for the adsorption of methylene blue [2]. Applications of activated carbon include air and water purification, water filtration, ground water remediation, adsorption of poisons, and drug overdoses. These and several other reasons are behind its increased market demand. According to [3], its preparation involves carbonization of the precursor below 800°C in an inert atmosphere before carbonization. In this research, coconut shells were used because they are cheap and readily available in Nigeria. The shells contain volatile matter and moisture that are removed by the application of heat [4]. Gratuito et al. [5] carried out process optimization of activated carbon yield produced from coconut shells using RSM. Different methods are available for producing activated carbon but for specific industrial application, a solid adsorbent with wide pore size distribution can be preferably obtained via chemical activation [6]. Activated carbons obtained from snail shells and apple peels were discussed [6, 7]. Hung [8] used a fluidized bed reactor to convert crushed coconut shells to activated carbon, syngas, bio-oils, and water while, in [9], bamboo was used to prepare activated carbon of high surface area. The various methods for preparing activated carbon from carbon precursors are contained in [10]. Karacan et al.

[11] optimized the manufacturing conditions for producing activated carbon from lignite. Ketcha et al. [12] prepared activated carbon from maize cobs using zinc chloride as activating agent. The reduction of hexamine III cobalt was carried out using activated carbon produced from coconut shells as catalyst [13], while the work of Mourao et al. [14] considered the influence of oxidation on the adsorptive capacity of activated carbon synthesized from lignocellulosic precursors. The preparation and characterization of activated carbons from cellulosic waste materials for waste water treatment were carried out [15–17]. Before carbonization, the raw materials are impregnated with chemicals such as acid, strong base, or salt [18]. Production and characterization of activated carbons from coconut shells were discussed [19]; their adsorption capacities were determined by contacting them separately with methyl red and potassium permanganate. Shalna and Yogamoortthi [20] produced activated carbon with high chromium removal efficiency from tea dust using H_3PO_4 as the activating agent. Sodeinde [21] used activated carbon produced from coconut shells impregnated with $ZnCl_2$ to obtain cobalt II from cobalt III, and the results were similar to those of Long et al. [13]. Bagasse, apricot stones, hazelnut, almond, pistachio, and walnut hard shells when used as precursors for producing activated carbon show that activation temperature/time and chemical-to-carbon impregnation ratio are important parameters for determining the quality of activated carbon [22]. Coconut fibre was used for synthesizing activated carbon using H_3PO_4 as activating agent [23]. Several works on synthesis of activated carbon via chemical activation involve the use of popular chemicals such as H_3PO_4, $ZnCl_2$ and KOH as activating agents; however, H_3PO_4 is preferred to $ZnCl_2$ because of the adverse effect $ZnCl_2$ has on the environment, hence the reason for its limitation in use in the food and pharmaceutical industries [24]. The use of other raw materials such as rubber, wood dust [24], and sugar cane bagasse pith [25] has also been exploited as raw materials for producing activating carbon. Tan et al. [26] also conducted an optimization study on activated carbon produced from coconut husk which was found suitable for the removal of 2,4,6-trichlorophenol using KOH treatment and CO_2 gasification. This paper focuses on determining the optimum temperature and concentration for the synthesis of activated carbon with excellent adsorptive performance using DRM since previous works had their intents on obtaining the best activating agent, carbon yield, carbon-to-chemical impregnation ratio, and so forth. The mathematical approach widely used is RSM. Till date, no research work states the optimum temperature and concentration(s) of H_3PO_4 required for producing one or more varieties of coconut shell activated carbon; again, this brings to mind the need to find out if the optimum conditions for producing activated carbon with excellent adsorptive performance is the same for separate varieties of coconut shells.

2. Equipment, Materials, and Reagents

2.1. Raw Materials, Chemicals, and Reagents. The materials and reagents used include coconut shells from tall and dwarf trees, distilled water, 0.3 M, 0.5 M, 0.67 M, and 1.33 M concentrated phosphoric acid of 99% purity manufactured by Sigma-Aldrich, 95% pure zinc chloride pellets made by MRS Scientific Ltd., 1 M KOH of 85% purity, made by Sigma-Aldrich and methylene blue dye, buffer solutions 4.01 ± 0.02 (colour-coded pink, HACH 22835-48, 1 L) and 7.01 ± 0.02 (colour-coded yellow, HACH 22835-49, 0.5 L) for pH meter calibration made by HM Digital Inc., USA, measuring cylinder, flat bottom flasks, conical flask, and beakers manufactured by J Sill Borosilicates, and filter paper by Whatman No. 2V and of 18 cm diameter.

2.2. Instrumentation and Equipment. Automated sieve shaker by Matest-Treviolo (for sieving particles of coconut shells), Italy, UV mass spectrophotometer: 7310 visible Scanning Spectrophotometer fitted with 10×10 mm cuvette holder, 320–1000 nm wavelength, resolution = 1 nm accuracy of ±2 nm, manufactured by Jenway (used to measure the transmittance and absorbance of filtrate/unabsorbed dye solution), muffle furnace with maximum temp. of 1300°C and 5–23 L chamber volume, made by Carbolite Gero (for heating the samples/carbonization), Oven Vs-1202d3 made by Vision Scientific Co. Ltd. (for drying the samples), electronic weighing balance manufactured by Swastic Systems and Services, India (used to measure the weights of samples), pH meter (used to determine the pH of the activating agents and activated carbons), Orion™ Dual Star™ pH, ISE Mv, ORP with temperature dual channel bench top meter manufactured by Thermo Fisher Scientific, and Joel Field Emission Electron Microscope JESM-7600F were used to obtain the elemental compositions of the activated carbons and visualize the surfaces of the samples.

2.3. Mathematical Determination of Optimization Boundaries. The Differential Response Technique was used to establish the experimental conditions and parameters of interest include carbonization temperature X_1 and concentration of reagent X_2 towards obtaining activated carbon of high adsorption capacity and economic viability. Central composite design was used to determine the minimum number of experiments required. We then calculated N using

$$N = 2n + 2n + nc = 2(1) + 2(1) + 0 = 4, \qquad (1)$$

where N is the total number of experiments required, nc is center runs ($nc = 0$), and n is the number of factors ($n = 1$). Hence, for minimum experimental runs, N is given as 4.

We modified the factorial design propounded by Karacan et al. [11]:

$$Y = b_0 + b_1 X_1 + b_2 X_2 + b_3 X_3 + b_4 X_1 X_2 + b_5 X_1 X_3 \\ + b_6 X_2 X_3 + b_7 X_1 X_2 X_3, \qquad (2)$$

where Y is the yield, b_0 is the global mean, and b_i represents the other regression coefficients, where $i = 1, 2, 3, \ldots, j$.

The model formulation depends on carbon yield because it is common to all variables. The number of terms equals the number of experiments; hence

$$Y = b_0 + b_1 X_1 X_2 + b_2 (X_1 X_2)^2. \qquad (3)$$

For every difference in yield $(Y + \Delta Y)$, it is as a result of an increase in the input variables $(X_1 + \Delta X_1)$ and $(X_2 + \Delta X_2)$, therefore,

$$(Y + \Delta Y) = b_0 + b_1 (X_1 + \Delta X_1)(X_2 + \Delta X_2)$$
$$+ b_2 ((X_1 + \Delta X_1)(X_2 + \Delta X_2))^2. \tag{4a}$$

Subtract (3) from (4a)

$$\Delta Y = b_1 X_2 \Delta X_1 + b_1 X_1 \Delta X_2 + b_1 \Delta X_1 \Delta X_2$$
$$+ 2b_2 X_1^2 X_2 \Delta X_2 + b_2 X_1^2 \Delta X_2^2 + 2b_2 X_1 X_2^2 \Delta X_1$$
$$+ 4b_2 X_1 X_2 \Delta X_1 \Delta X_2 + 2b_2 X_1 \Delta X_1 \Delta X_2^2 \tag{4b}$$
$$+ b_2 X_2^2 \Delta X_1^2 + 2b_2 X_2 \Delta X_1^2 \Delta X_2$$
$$+ b_2 \Delta X_1^2 \Delta X_2^2.$$

Divide through by ΔX_1 and set $\Delta X_1 \rightarrow 0$. The above equation then gives

$$\frac{dY}{dX_1} = b_1 (X_2 + \Delta X_2)$$
$$+ b_2 \left(2X_1 X_2^2 + 4X_1 X_2 \Delta X_2 + 2X_1 \Delta X_2^2\right), \tag{5}$$

$$\frac{d^2Y}{dX_1^2} = b_2 \left(2X_2^2 + 4X_2 \Delta X_2 + 2\Delta X_2^2\right)$$
$$= 2b_2 (X_2 + \Delta X_2)^2. \tag{6}$$

We take the second differential equation by dividing (4a) through by ΔX_2 and set $\Delta X_2 \rightarrow 0$.

$$\frac{dY}{dX_2} = b_1 (X_1 + \Delta X_1)$$
$$+ b_2 \left(2X_2 X_1^2 + 4X_1 X_2 \Delta X_1 + 2X_2 \Delta X_1^2\right), \tag{7}$$

$$\frac{d^2Y}{dX_2^2} = b_2 \left(2X_1^2 + 4X_1 \Delta X_1 + 2\Delta X_1^2\right)$$
$$= 2b_2 (X_1 + \Delta X_1)^2.$$

From (5),

$$\frac{d^2Y}{dX_1 X_2} = b_1 + b_2 \left(4X_1 X_2 + 4X_1 + 2X_1 \Delta X_2\right). \tag{8}$$

From (6),

$$\frac{d^2Y}{dX_2 X_1} = b_1 + b_2 \left(4X_1 X_2 + 4X_2 + 2X_2 \Delta X_1\right). \tag{9}$$

The coefficients in (5)–(9) above act as normalizing agents. The optimum condition for minimum experimental runs is very difficult to draw conclusions from; however, the DRT has the ability to monitor minute changes. The solution of (9) was chosen because of the role of concentration of chemical reagent for minimum experimental runs. However, we recommend the solutions of (5)–(8) for higher experimental runs. For economic reasons, few experimental runs were considered as they help to understudy the weaknesses and strengths of the approach adopted.

3. Method

3.1. Procedure. The procedure for preparing the activated carbon samples is discussed as follows.

3.1.1. Preparation of the Raw Material. Coconut shells of the West African tall tree variety, about 90 ft tall, were collected from Okiewo in Edo state, Nigeria. To remove moisture, they were sun-dried for 3 days. The shells were pulverized and sieved using the 0.15 mm size sieve of the automated sieve shaker in order to obtain uniform fines with increased surface area.

3.1.2. Dye Solution for Adsorptive Performance Test. Methylene blue dye solution was used to test the performance of the activated carbons.

3.1.3. Calibration Curve for Methylene Blue. To test for the adsorptive performance of the activated carbon samples, a produced activated carbon sample was mixed with a 50 mL fixed concentration of methylene blue dye solution at 1 g/L for 2 hours. The mixture was filtered and the filtrate was then analysed using a UV/Vis spectrophotometer to get the absorbance of dye solution. Different concentrations of dye solutions in the range of $1 \, \text{mgL}^{-1}$ to $1000 \, \text{mg L}^{-1}$, as shown in Table 1, were prepared. They were each mixed with equal portions of the produced activated carbon. The mixtures were filtered and the filtrates were analysed using a UV/Vis spectrophotometer. A calibration graph (plot of absorbance against residual concentration of methylene blue solution, Beer Lambert's plot) was then obtained from which the absorbance of each activated carbon sample was determined. From (10), the adsorptive capacities of the activated carbon samples were calculated:

$$\text{adsorptive capacity (\%)} = \frac{C_o - C}{C_o} \times 100, \tag{10}$$

where C_o is the initial concentration of dye; C is the concentration of dye after adsorption.

3.2. Experiments

3.2.1. Experiment 1

Effect of Chemical Agent on Activated Carbon Performance and Yield. 100 mL solutions of 1 M $ZnCl_2$, KOH, and H_3PO_4 having pH of 5.26, 11.18, and 3.0 at 29°C, respectively, were prepared. Three 7 g portions of the coconut shell samples prepared in Section 3.1.1 were weighed, mixed, and soaked for 24 hours in the $ZnCl_2$, KOH, and H_3PO_4 labelled S_1, S_2, and S_3, respectively. They were kept in an oven to dry at 105°C. The samples were then heated in a muffle furnace at 575°C. After one hour, the samples were washed with distilled water to remove the residual inorganic matter and excess chemical agent after which they were dried again in the oven at 105°C for 24 hours.

Another sample labelled S_4 (NAC), that is, coconut shell without any form of chemical impregnation, was prepared by the method described above.

TABLE 1: Concentration variation with absorbance for the methylene blue solutions, methylene blue wavelength (665 nm).

Concentration (mg/L)	Absorbance
0	0
1	0.263
2	0.412
10	1.424
25	1.595
50	1.653
100	1.727
125	1.754
250	1.842
375	1.909
500	1.959
625	1.992
750	2.051
1000	2.153

The produced activated carbons from samples S_1, S_2, S_3, and S_4 were then weighed to evaluate their carbon yields. Thereafter, the procedure in Section 3.1.3 was used to determine the absorbance of the filtrates by adding 50 mL of the methylene blue dye prepared with the activated carbon for 2 hours and (10) was used to obtain their adsorption capacities.

3.2.2. Experiment 2

Effect of Concentration of Chemical Agent on Activated Carbon Performance and Yield. H_3PO_4 was chosen for this experiment because the sample activated with H_3PO_4 in Experiment 1 gave the best adsorptive performance; see Table 5. Five solutions of 0.3 M, 0.5 M, 0.67 M, 1.00 M, and 1.33 M of the acid were made. Five separate 7 g portions of the tall tree coconut shell samples were soaked separately in 100 mL of 0.3 M, 0.5 M, 0.67 M, 1 M, and 1.33 M H_3PO_4 having pH of 2.2, 2.17, 2.07, 1.98, and 1.96 at 29°C, respectively, for 24 hours. The samples were then labelled A_1, $A_{1.5}$, A_2, A_3, and A_4, respectively, before being heated in the oven at 105°C.

In order to find out if the optimum concentration of H_3PO_4 for producing a very good activated carbon is general for all coconut varieties, shells from a Malayan Yellow Dwarf Variety sourced from Warri area of Delta State Nigeria were also collected, prepared, and processed to yield activated carbon using the procedure in Section 3.1.1 and the adsorptive performances of the carbon samples were determined using the method described in Section 3.2.1 but, here, four parts of the shells obtained from the dwarf variety each weighing 7 g were processed using 100 mL 0.3 M, 0.67 M, 1 M, and 1.33 M H_3PO_4, respectively. The samples were labelled A_{1*}, A_{2*}, A_{3*}, and A_{4*}; see Tables 4 and 5 for the yields and adsorptive performance (as described in Section 3.2.1) of the activated carbon samples, respectively.

3.2.3. Experiment 3

Effect of Carbonization Temperature on Activated Carbon Performance and Yield. Four separate 100 mL solutions of

0.67 M H_3PO_4 having a pH of 2.07 at 29°C were prepared; 0.67 M H_3PO_4 was selected for this experiment because, in Experiment 2, the activated carbon produced with 0.67 M H_3PO_4 gave the best adsorptive performance.

Four parts of coconut shell samples were weighed and soaked in 100 mL of the four solutions for 24 hours. The first three samples labelled B_1, B_2, and B_3 weighed 7 g each while the last sample (B_4) weighed 6.2 g. The samples were dried in the oven at 105°C. The samples were placed in the muffle furnace for carbonization at 450°C (B_1), 575°C (B_2), 700°C (B_3), and 850°C (B_4) for 1 hour. The procedure in Section 3.2.1 was repeated so as to evaluate the yield of the activated carbon. In order to determine the adsorptive capacity of the carbon samples, the procedure in Section 3.1.3 was repeated using 50 mL dye solution at 2 hours of adsorption time.

3.2.4. Experiment 4

Effect of Chemical Agent on Physicochemical Properties of the Activated Carbon. In this experiment, the best tall tree variety activated carbon in Section 3.2.3 and commercial activated carbon (CAC) samples were tested for their moisture, ash, and volatile matter contents. Each sample was weighed and carbonized in the muffle furnace at 600°C for 1 hour; the properties were found as follows.

(i) Moisture Content. The mass of empty crucible with lid (m_1) was first measured and recorded. The sample was then placed in the crucible and the total mass m_2 was measured. The crucible with sample in it but with its lid removed was heated in an oven at 150°C. After 3 hours, the crucible was covered with its lid and the total mass m_3 was measured. Equation (11) was used to calculate the percent moisture removed from each sample:

$$\text{moisture content (\%)} = 100\% \times \frac{(m_1 - m_2)}{(m_1 - m_3)}, \qquad (11)$$

where m_1 is the mass of empty crucible with lid (g); m_2 is the mass of crucible with lid and sample (g); m_3 is the mass of crucible, lid, and dried sample (g).

(ii) Ash Content. Some of the sample that gave the best result in Section 3.2.3 was placed in an open crucible of mass m_4 and the total weight was recorded as m_5. The sample was placed in a muffle furnace whose temperature was adjusted to 650°C. After 3 hours, the resultant weight m_5 of the crucible and contents was recorded. Using (12), the ash content of the activated carbon sample was obtained:

$$\text{ash content (\%)} = 100\% \times \frac{(m_6 - m_4)}{(m_5 - m_4)}, \qquad (12)$$

where m_4 is the mass of empty crucible in (g); m_5 is the mass of crucible plus original sample in (g); m_6 is the mass of crucible plus ash in (g).

(iii) Volatile Matter Content. Some of the sample with best results in Section 3.2.3 was transferred into a crucible of mass
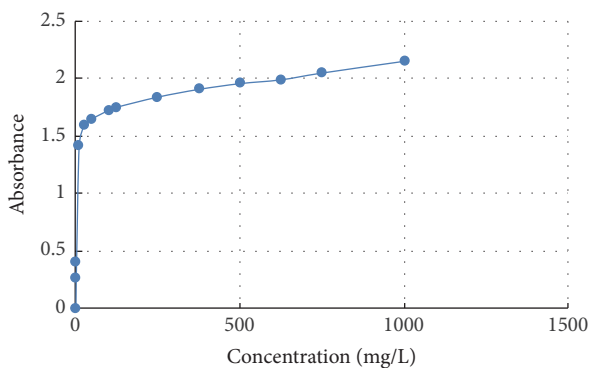
FIGURE 1: Absorbance versus concentration of the methylene blue dye.

m_4 and covered with lid; the total weight was recorded as m_7. The crucible with sample in it was then placed in the muffle furnace whose temperature was adjusted to 900°C. After 7 minutes, the crucible was removed, allowed to cool, and reweighed; the mass was recorded as m_8. The volatile matter content of the activated carbon was obtained from

volatile matter content (%)

$$= 100\% \times \frac{[100\,(m_7 - m_3) - m_c\,(m_7 - m_8)]}{(m_7 - m_3)\,(100 - m_c)}, \tag{13}$$

where m_7 is the mass in g of the crucible, lid, and sample before heating; m_8 is the mass in g of the crucible, lid, and content after heating; m_3 is the mass in g of the empty crucible and lid; m_c is the percentage by mass of moisture in the sample.

3.2.5. Surface Morphology and Elemental Compositions of Activated Carbons.
The scanning electron microscope (JESM-7600F) was used to visualize the surfaces of the samples. The samples prepared were mounted on a double-sided carbon tape. The samples were exposed to an electron beam at an accelerating voltage of 15 keV in order to obtain a signal for the SEM studies. The micromarker on the micrographs was used to estimate the pore size (diameter). The elemental composition, which is given in both atomic percent and weight percent that reflects the amount of a particular element in the analysed volume, was obtained with SEM.

4. Results and Discussion

4.1. The Calibration Curve.
The calibration curve was drawn using the method discussed in Section 3.1.3 at a wavelength of 665 nm. In Table 1, concentration of dye in the samples increased with absorbance and the highest absorbance was recorded for the 1000 mg L^{-1} solution. Figure 1 partly obeys Beer Lambert's law which states that a linear relationship exists between absorbance and concentration, although the law has conditions for nonlinearity especially for concentrations greater than 0.000001 M. The lowest concentration in
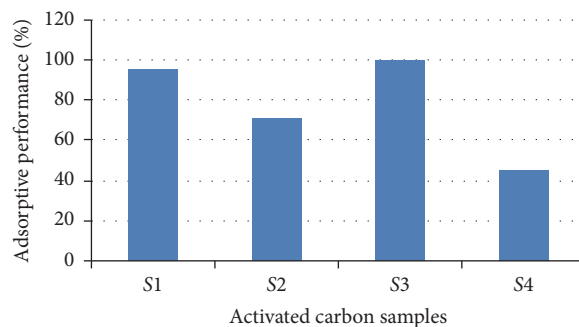

FIGURE 2: Adsorptive performance for activated carbon.

TABLE 2: Effect of activating agent on adsorptive performance.

Sample	Activating agent	Absorbance	Adsorptive performance (%)
S1	ZnCl$_2$	1.661	94.9
S2	KOH	1.87	70
S3	H$_3$PO$_4$	0.166	99.9
S4	Nil	1.903	45

the calibration curve of Figure 1 is 1 mgL^{-1} which is equivalent to 0.0000031 M; hence, a nonlinear plot was obtained.

4.2. The Effect of Activating Agent on the Carbon.
The effect of activating agent was determined in order to ascertain the following.

4.2.1. Adsorptive Performance.
In Table 2 and Figure 2, the sample with the highest absorbance and adsorptive performance is S_4, that is, the NAC. Sample S_3 gave the least absorbance but the highest adsorptive performance of 99.9%, hence, the most efficient adsorbent for methylene blue dye. Sample S_3 gave the best adsorptive performance followed by S_1 because the H$_3$PO$_4$ and ZnCl$_2$ impregnated samples may have resulted in better developed pores compared to other samples at the stated conditions. H$_3$PO$_4$ in carbon precursors splits cellulose fibres and depolymerizes lignin and hemicellulose which results in mechanical resistance decline of the particle, inflammation of the material, and more cross-linked aromatic products. Additional cross-linking may be induced by the presence of phosphates [17]. ZnCl$_2$ exhibits Bronsted-acidity; hence, it donated protons to the particle which helped to break down the cellulose and lignin structures of the particle. Inflammation of the particles occurred as a result of the degradation; hence, there was reduction in mechanical resistance of the carbon particles. The presence of ZnCl$_2$ and H$_3$PO$_4$ in the interior of the particles during carbonization gave rise to some degree of resistance to contraction of their pore volumes.

It was suspected that KOH did not react at the 575°C; hence, it could not restrain the shrinking of the pore volume of the carbon particle. In addition, the porous structure of the sample was not well developed compared to those of

TABLE 3: Effect of activating agent on activated carbon yield.

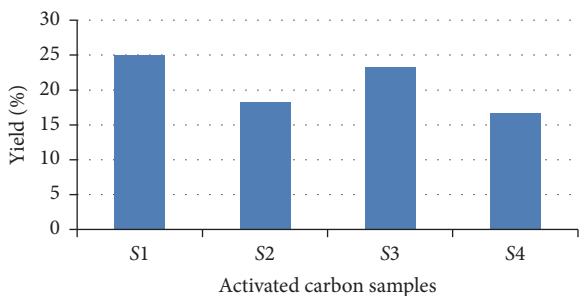| Sample	Activating agent	Yield (%)
S_1	$ZnCl_2$	25
S_2	KOH	18.3
S_3	H_3PO_4	23.3
S_4	Nil	16.7

FIGURE 3: Chemical agent versus activated carbon yield.

samples S_1 and S_3. Also, the particles pore volume could have been blocked by products of decomposition which reduced its adsorptive capacity.

4.2.2. Activated Carbon Yield

(i) Effect of Type of Chemical Agent on Yield. In Table 3, sample S_1 gave the highest yield of 25% because it underwent the most efficient dehydration during carbonization. For carbonization to be highly effective, complete removal of oxygen and hydrogen is necessary. The degree of conversion of the precursor to carbon varies because of the loss of some amount of carbon with oxygen and hydrogen as CO_2, CO, or hydrocarbons. In S_1, the $ZnCl_2$ fosters the removal of hydrogen and oxygen probably as water leaving behind the carbon atoms. According to [17], a typical lignocellulosic material comprises about 48% carbon. The highest yield of 25% was obtained probably because of several factors including the carbonization temperature and the $ZnCl_2$ concentration used. Closest to the yield of S_1 is the yield from sample S_3 due to their similar dehydrating effect on the precursor; see Table 3 and Figure 3.

18% yield was obtained for the KOH impregnated sample. The NAC sample gave the lowest yield because there was no dehydrating agent in the sample leading to loss of more carbon atoms along with hydrogen and oxygen; see Figure 3.

4.3. Effect of Activating Agent Concentration. The effect of activating agent concentration on activated carbon yield was obtained and the results are as seen in Table 4.

4.3.1. Effect of Activating Agent Concentration on Activated Carbon Yield. In Table 4, the sample impregnated with 1 M H_3PO_4 gave the highest activated carbon yield while the sample impregnated with 0.3 M of the acid gave the lowest yield for both samples, although that of the dwarf variety is

higher; see Table 4. Figure 4(a) shows the variation of the activating agent concentration with activated carbon yield.

For the activated carbon samples A_{1*}, A_{2*}, A_{3*}, and A_{4*}, the yield of the activated carbon also increased with increased concentrations of H_3PO_4; see Table 4. The value recorded for 1.33 M acid concentration (A_{4*}) is 40.1% which is 6% higher than the carbon yield obtained with 1 M concentration of H_3PO_4. The trend observed can be likened to the dehydrating effect of H_3PO_4 on the precursors during carbonization. Also, samples with higher concentrations of H_3PO_4 up to 1.33 M lost more atoms of oxygen and hydrogen extracted as water causing an increase in the activated carbon yield.

For sample A_{4*}, the yield was less by 6% when compared to that of A_{3*}; thus, the optimum H_3PO_4 concentration for preparing activated carbon of high yield, with little attention on performance for both species, is 1 M based on the findings of this study; see Table 4.

4.3.2. Effect of Activating Agent Concentration on Adsorptive Performance of Activated Carbon. Based on the DRT, (9) was used to simulate the optimum conditions discussed in Figures 4(b) and 4(c). Figure 4(b) shows an optimization process when temperature controls the chemical reaction. The variation between 0.3 M and 0.97 M shows that processing activated carbon within this concentration range may positively increase the expected carbon yield; this agrees with the experimental results. The results in Figure 4(c) show that concentration may not have positive influence on the yield if further increased. Again, this agrees well with our experiment since, for the tall tree variety, the sample with the best adsorptive performance is the sample impregnated with 0.67 M H_3PO_4 as described in Section 3.2.2; hence this is the reason it was chosen for the analysis. The carbonization temperature for all samples was 575°C and the activation time was 1 hour. A_1, $A_{1.5}$, A_2, and A_3 were the activated carbon samples produced using H_3PO_4 impregnation at 0.3 M, 0.5 M, 0.67 M, and 1 M concentrations, respectively. However, in Table 5, samples A_2 and $A_{1.5}$ gave the best adsorptive performance of 100% with corresponding absorbance of 0.04 and 0.07, respectively, whereas, for samples A_{1*}–A_{4*} of the dwarf variety, the sample with the best adsorptive performance was sample A_{3*} with adsorptive performance of 99.9% and absorbance of 0.76. While the operating conditions remain unaltered, in order that the adsorptive capacity of the activated carbon is maximized, the acid concentration must be kept between 0.3 and 0.67 M for the tall tree sample but between 0.3 and 1 M for the dwarf variety because the activated carbon pore structure tends to be destroyed or expanded above the stated concentrations of H_3PO_4 which in turn reduces their adsorptive capacities; see Figure 5. Again, for the tall tree variety, sample A_3 shows the highest absorbance but least performance. Absorbance is higher for sample A_1 than A_2. Therefore, the adsorptive performance increased with acid concentration from 0.3 to 0.67 M. The lower performance of sample A_3 may be due to excessive breakdown of the cellulose structure which may cause very little or no modification in the micropores at 575°C. Figures 7(a) and 7(b) give an overview of B1 and its pore size distribution as obtained from SEM analyses.
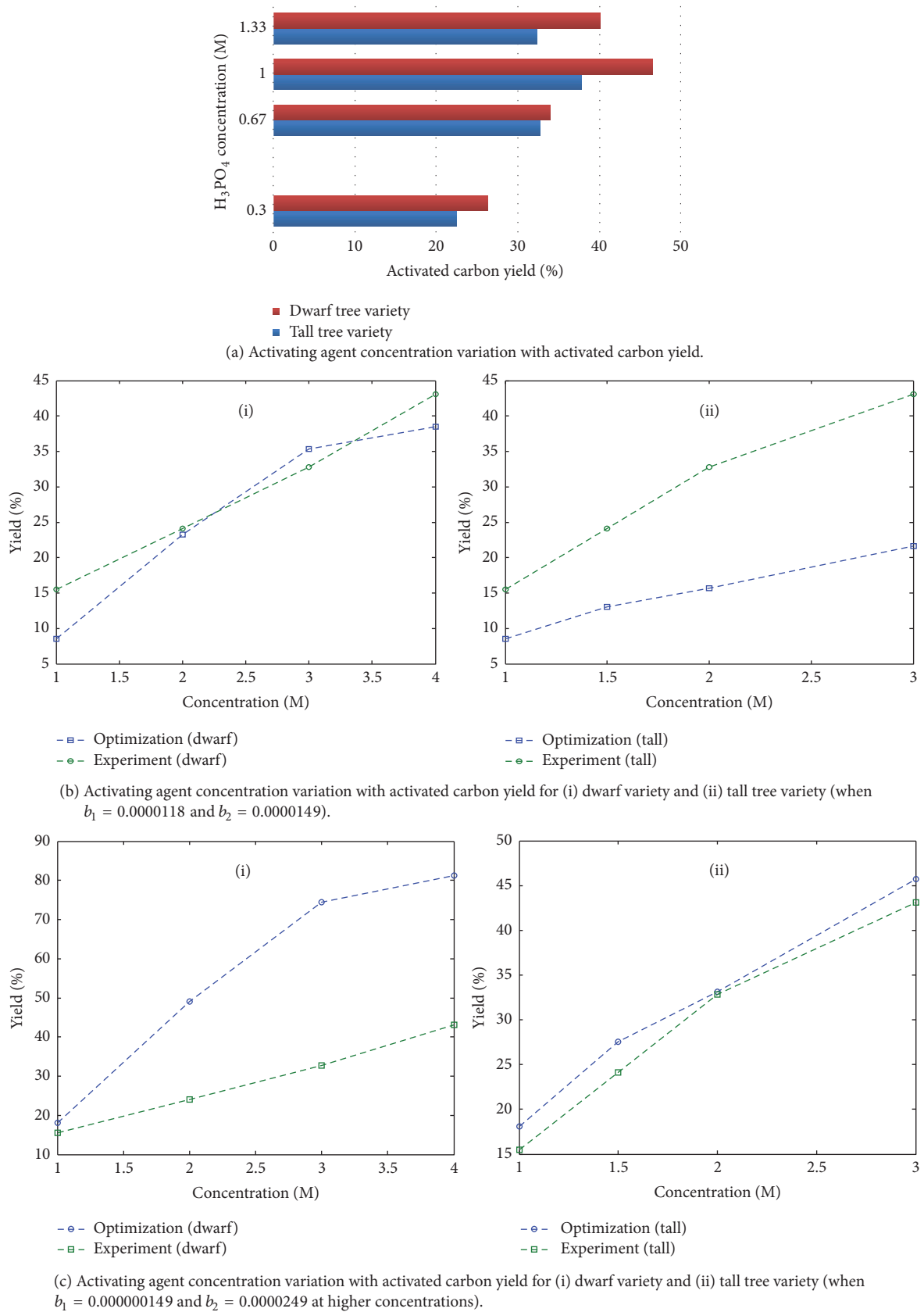
(a) Activating agent concentration variation with activated carbon yield.

(b) Activating agent concentration variation with activated carbon yield for (i) dwarf variety and (ii) tall tree variety (when $b_1 = 0.0000118$ and $b_2 = 0.0000149$).

(c) Activating agent concentration variation with activated carbon yield for (i) dwarf variety and (ii) tall tree variety (when $b_1 = 0.000000149$ and $b_2 = 0.0000249$ at higher concentrations).

FIGURE 4

TABLE 4: Effect of activating agent concentration on activated carbon yield.

Samples	H_3PO_4 concentration (M)	Tall tree variety yield (%) ($A1$–$A4$) at 575°C	Dwarf tree variety yield (%) ($A1*$–$A4*$) at 575°C
A_1, A_{1*}	0.30	22.4	26.3
$A_{1.5}$,—	0.50	24.1	—
A_2, A_{2*}	0.67	32.8	34.0
A_3, A_{3*}	1.00	37.9	46.6
A_4, A_{4*}	1.33	32.3	40.1

TABLE 5: Effect of activating agent concentration on absorbance and adsorptive performance.

Sample	H_3PO_4 concentration (M)	Absorbance	Adsorptive performance (%)
A_1, A_{1*}	0.30	0.116, 2.29	99.9, 97
$A_{1.5}$, —	0.50	0.066	100, —
A_2, A_{2*}	0.67	0.04, 1.76	100, 99.7
A_3, A_{3*}	1.00	1.707, 0.77	91.5, 99.9
A_4, A_{4*}	1.33	2.36, 3.187	80.2, 71.4

TABLE 6: Variation of temperature with activated carbon yield for tall tree variety.

Sample	Carbonization temperature (°C)	Performance (%)	Yield (%)
B_1	450	99.8	43.1
B_2	575	100.0	32.8
B_3	700	94.8	24.1
B_4	850	94.8	15.5
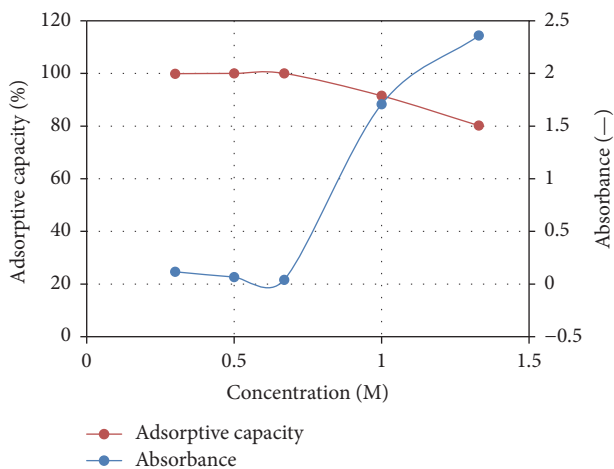
FIGURE 5: Profile of concentration of H_3PO_4 with absorbance and adsorptive performance samples.

4.4. The Effect of Carbonization Temperature on Activated Carbon Yield

4.4.1. Effect of Carbonization Temperature on Adsorptive Performance of Carbon.

In Experiment 3, all samples were impregnated with 0.67 M concentration of H_3PO_4. Table 6 shows the results obtained for the different samples. There was a slight increase in the adsorptive performance from 99.8% to 100% due to an increase in the carbonization temperature from 450°C to 575°C. At 575°C, it could be seen that the results from the scanning electron microscope (SEM) analysis show that more defined/finer pores were formed leading to a higher internal surface area and improved adsorptive properties of B_2; see Figures 8(a) and 8(b) for the structural morphology and pore size distribution of B_2 (i.e., in the range of 0.62 μm–1.76 μm) as compared to the morphology and pore size distribution (i.e., in the range of 0.73–2.57) for B_1. Also, a decrease in the adsorptive performance of the activated carbon from 100% to 94.8% was observed for samples B_3 and B_4, with pore sizes in the range of 0.68–1.50 μm and 0.77–3.77 μm, respectively, for an increase in the carbonization temperature from 575°C to 850°C; see Figures 9(a) and 9(b) and Figures 10(a) and 10(b) for the structural morphologies and pore size distributions of the activated carbons formed at both temperatures, respectively. This may be due to excessive carbonization causing distortion or further expansion of other pore walls between successive neighbouring pores. Furthermore, the phosphate and polyphosphate links formed during the condensation reaction become volatile above 650°C which makes it difficult for these compounds to be able to inhibit contraction of the pore volume thus, giving a decrease in porosity and adsorptive characteristic of the particle.

For the dwarf variety, sample A_{3*} gave even pore size distribution, that is, 1.80 μm, while for sample A_4 the pore size distribution is in the range of 0.53–0.68 μm; see Figures 11(a) and 11(b) and 12(a) and 12(b) respectively, for their morphologies and pore size distributions.

4.4.2. Effect of Carbonization Temperature on Activated Carbon Yield.

In Table 6 and Figure 6(a), the activated carbon yield reduced at temperatures above 450°C; the same can be seen in Figure 6(b). The decrease in yield was as a result of the expulsion of phosphate compounds and volatile matter from the samples and this is in agreement with the results
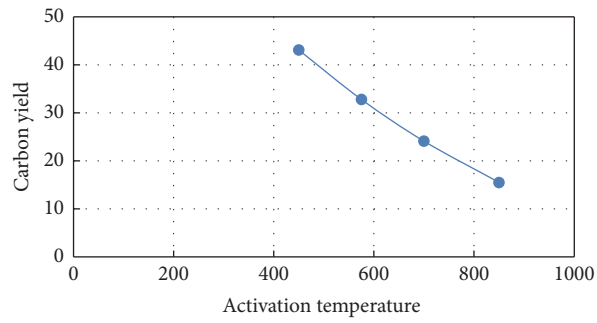
(a) Carbonization temperature variation with carbon yield for the tall tree variety.
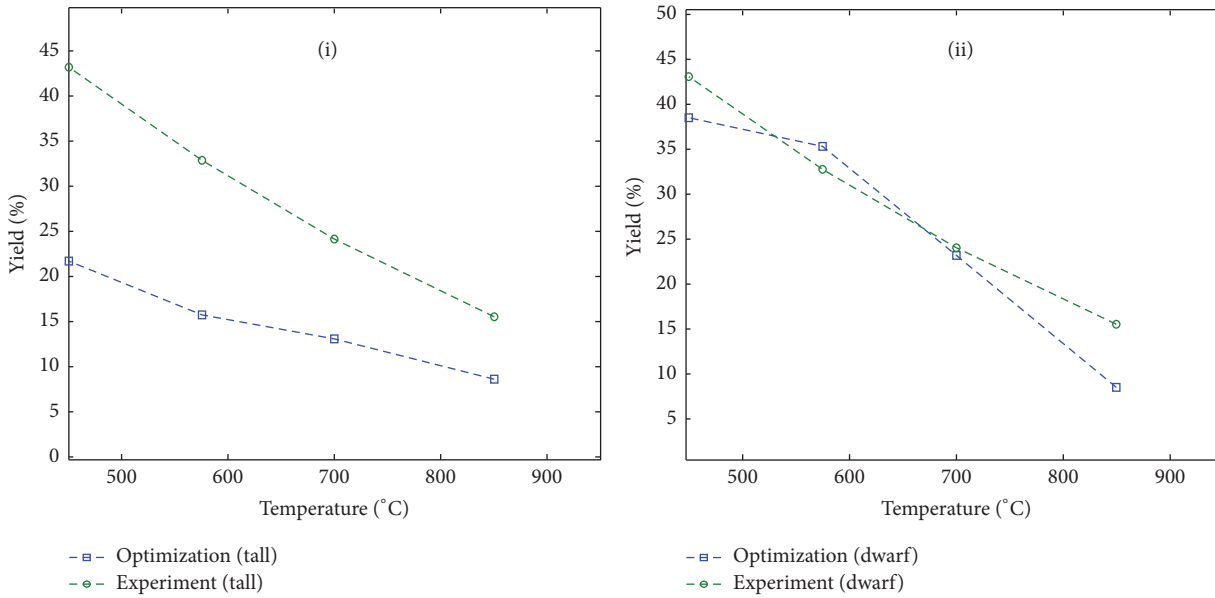
(b) Carbonization temperature variation with carbon yield for (i) tall tree variety and (ii) dwarf variety (when $b_1 = 0.0000118$ and $b_2 = 0.0000149$).
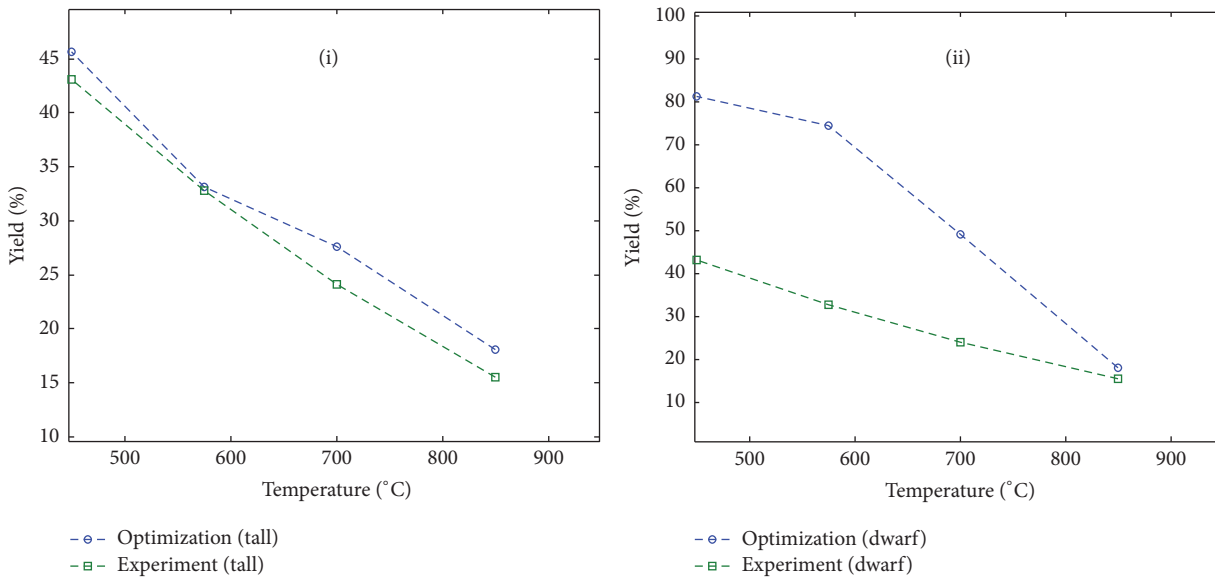
(c) Carbonization temperature variation with carbon yield for (i) tall tree variety and (ii) dwarf variety (when $b_1 = 0.000000149$ and $b_2 = 0.0000249$).
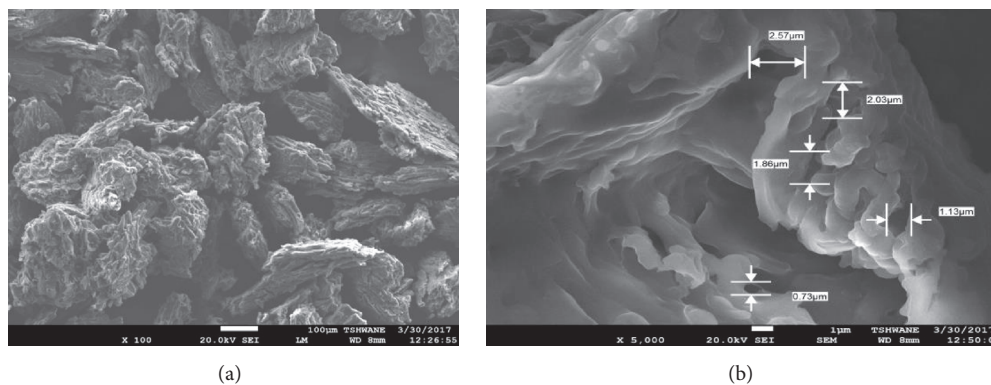
FIGURE 6

(a)   (b)

FIGURE 7: (a) Overview of B_1 from SEM analysis; (b) pore size distribution of B_1 at ×5000 magnification.

TABLE 7: Adsorptive performance and absorbance of the synthesized and commercial activated carbons.

Material	Absorbance	Adsorptive performance (%)
Sample B_2	0.04	100
Commercial AC	0.023	100

TABLE 8: Physicochemical properties of the synthesized and commercial activated carbons.

Carbon sample	Moisture content, %	Ash content, %	Volatile matter, %
CAC	5	5.28	68.4
B_2	7	7.2	57

of Ip et al. [9]. Higher temperatures of 575 to 850°C alter the mesoporous and macroporous structures of the particles and under these conditions, the yield dropped to 15.5%; the highest yield was obtained at 450°C; hence, in order to maximize the yield, the carbonization temperature should be kept at 450°C which corresponds to an activated carbon yield of 43.1%.

In Figure 6(b), based on the model, the variation between 450°C and 850°C shows that processing activated carbon at higher temperatures will decrease the expected yield. We also considered a condition when concentration controls the chemical reaction; see Figures 4(b) and 4(c). This shows that concentration of the acid has influence on the yield if further increased which agrees well with the experimental data despite the slight deviations.

4.5. Comparing the Sample Activated Carbon with Commercial Activated Carbon. In Table 7, comparing B_2 and the CAC, a similar adsorptive performance of 100% is indicative of good product efficiency and quality, although the absorbance of the CAC is slightly lower which may be due to the type of activating agent, nature of precursor, carbonization temperature, and concentration of the active agent used to produce the CAC.

4.6. Physicochemical Properties of the Sample Activated Carbon. In Table 8, the physicochemical properties of the activated carbon B_2 obtained in Section 3.2.4 are shown with those of the NAC sample.

(i) Moisture Content. According to Indo German Carbons Limited, the moisture content of activated carbon should be ≤6%. Under standard conditions, moisture has no effect on the performance of activated carbon. The moisture content

of the NAC sample was 5% while that of B_2 was 7% because the H_3PO_4 used to impregnate the activated carbon sample was in its aqueous state which added more water to sample B_2.

(ii) Ash Content. B_2 gave ash of about 7.2% while the NAC gave 5.28% ash. This is because the phosphate compounds formed by the acid in B_2 increased the volume of the inorganic matter in the activated carbon thus increasing the amount of nonignitable residue left in the furnace. The smaller % ash in the NAC sample is likened to the lack of chemical agent within the precursor. Based on literature, the ash content of CAC is between 2 and 10%; hence that of B_2 is acceptable since high percent ash reduces the efficiency of reactivation/regeneration of activated carbons.

(iii) Volatile Matter. From the experiment, sample B_2 was seen to contain less volatile matter relative to the NAC whose values are 57% and 68.4%, respectively. Sample B_2 had lower volatile contents because H_3PO_4 forms phosphates and polyphosphate esters with hydrogen and oxygen atoms which would have been given off as gases during the carbonization process. Also, the dehydrating effect of the acid caused the water in the material to vaporize; hence, the covalent bond in the carbon matrix was therefore strengthened leaving no room for carbon loss. For the NAC sample, it lacked any chemical agent that could bring about those reactions. Also, the carbon matrix is weaker than that of sample B_2 which makes for possible loss of carbon atoms in gaseous forms.

The elemental composition of sample B_2 can be found in Table 9 which shows the percentage composition of the atoms in the activated carbon. The percentage atom of carbon in the sample is 88.46% and that of oxygen is 11.04% while
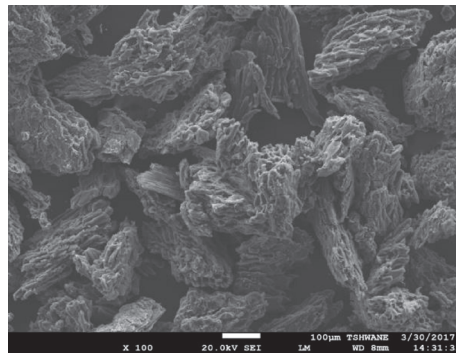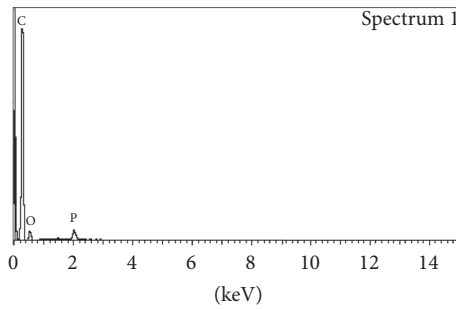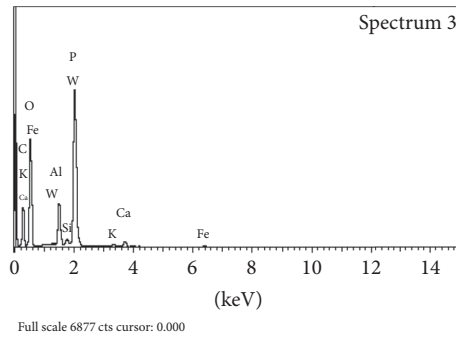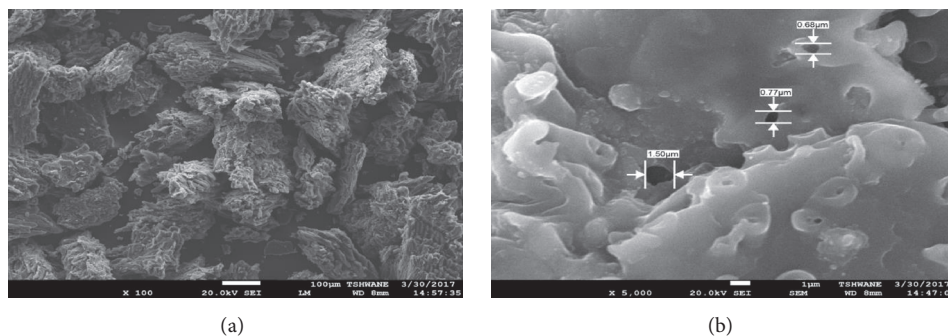
(a)
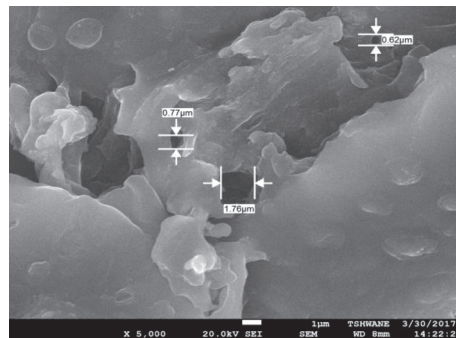
(b)

(a) Overview of B_2 from SEM analysis.

(b) Pore size distribution of B_2 at ×5000 magnification.

Full scale 6877 cts cursor: 0.000

(c)

Full scale 6877 cts cursor: 0.000

(d)

(c) Atomic spectrum of B_2 at 600 μm wavelength.

(d) Atomic spectrum of A_{3*} at 10 μm wavelength.

FIGURE 8

(a)

(b)

FIGURE 9: (a) Overview of B_3 from SEM analysis; (b) pore size distribution of B_3 at ×5000 magnification.
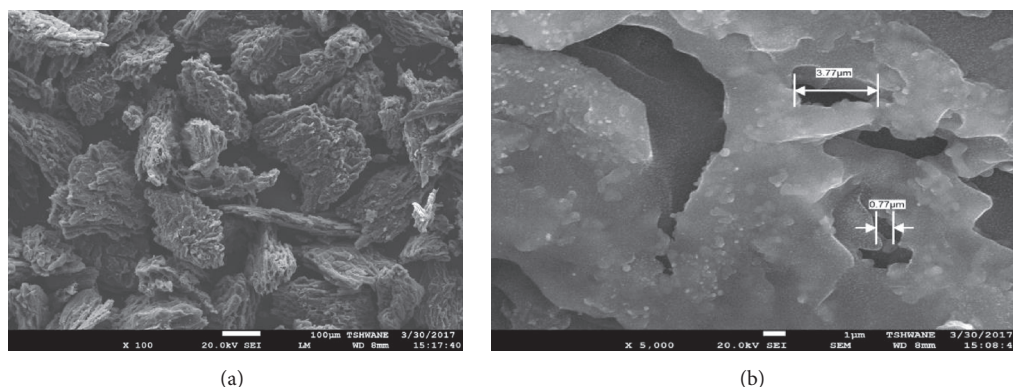

(a)

(b)

FIGURE 10: (a) Overview of B_4 from SEM analysis; (b) pore size distribution of B_4 at ×5000 magnification.

TABLE 9: Elemental composition of B_2.

Element	Weight%	Atomic%
C K	84.69	88.46
O K	14.07	11.04
P K	1.24	0.50
Total	100.00	100.00

for phosphorus trace amount, that is, 0.5%, was found; see also Figure 8(c) for the atomic spectrum of B_2 at 600 μm wavelength. Figure 8(d) shows the atomic spectrum of A_{3*} with percent weight of carbon, oxygen, aluminium, silicon, phosphorus, potassium, calcium, and iron of 36.85%, 45.53%, 2.82%, 0.27%, 12.72%, 0.2%, 0.57%, 0.56%, 0.36%, and 0.7%; that is, the amount of oxygen present is higher than the amount of carbon. Also, the sample can be seen to have high amount of impurities.

4.7. Solutions pH and pH of Activated Carbon. The pH values of the reagents used are as documented in Table 10. The degrees of acidities of the acid solutions are seen to increase with decreased pH. The optimum pH for 0.67 M concentration of the H_3PO_4 required for making activated carbon of excellent performance from the tall tree variety

coconut shell is 2.07 while that for the dwarf variety is 1.98. The pH of B_2 is 2.20 while that of A_{3*} is 2.08; these values are indicative of the medium/media for activation.

4.8. Statistical Analyses of Model. Statistical analyses of the performance of the model was carried out considering the model predictions shown in Figures 4(b)(i) and (ii), 4(c)(i) and (ii), 6(b)(i) and (ii), and 6(c)(i) and (ii). Table 11 shows that the confidence interval of the model predictions lies between 95 and 99% with the correlation coefficients of the model for concentration effect on yield in Figures 4(b) and 4(c)(i) in the range of 96–99%, while the correlation coefficients for effect of temperature variation on the yield for both varieties as shown in Figures 6(b) and 6(c)(i) and (ii), for both varieties as predicted by the model, are in the range of 96%–99%, which shows that the model predictions agree well with experimental data; see Tables 11 and 12.

5. Conclusion

Coconut shell activated carbon with excellent adsorptive properties can be produced using H_3PO_4 concentrations between 0.3 and 1 M. 0.67 M phosphoric acid gave the best adsorptive performance and absorbance for the activated carbon synthesized from the tall tree variety. Increase in carbonization temperature caused a decrease in the activated
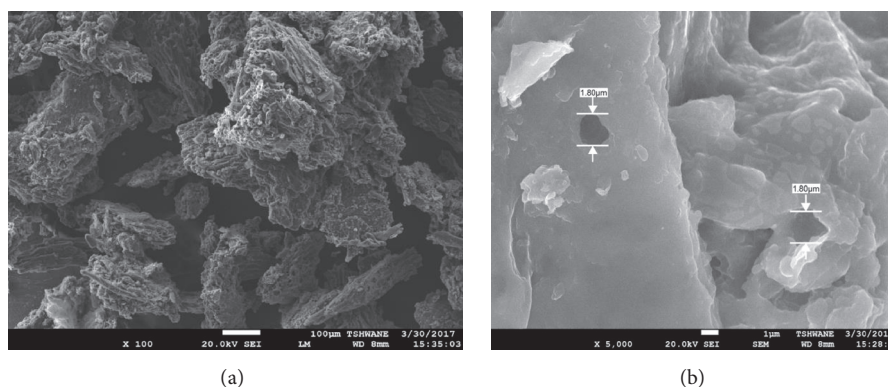
FIGURE 11: (a) Overview of A_{3*} from SEM analysis; (b) pore size distribution of A_{3*} at ×5000 magnification.
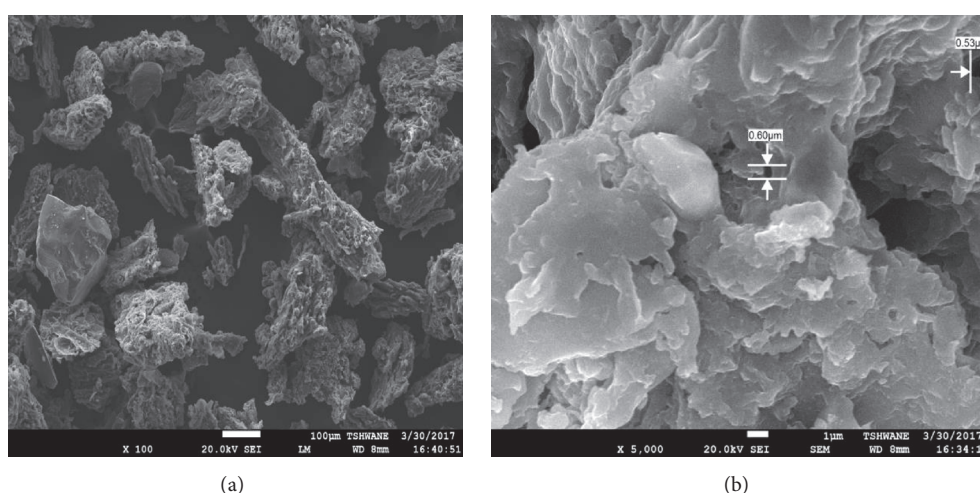

FIGURE 12: (a) Overview of A_{4*} from SEM analysis; (b) pore size distribution of A_{4*} at ×5000 magnification.

carbon yield. Activated carbon produced at 575°C gave the highest adsorptive performance of 100%. However, because of the relative difference (10%) in activated carbon yield of B_1 relative to B_2 and the slight variation of 0.2% in their adsorptive performances, the optimum temperature for producing activated carbon of the tall tree variety therefore lies between 450 and 575°C. The activating agents increased the ash and moisture contents of the carbon particles and decreased their volatile constituents. Based on the findings of this research, the optimum H_3PO_4 concentration and pH for preparing activated carbon of high yield from the tall and the dwarf variety coconut shells are 0.67 M and 2.07, respectively; higher concentrations above the optimum value gave lower yields for both varieties. The optimum temperatures were found to be in the range of 450–575°C for the tall tree variety coconut shell activated carbon, while, for the dwarf variety activated carbon, the optimum temperature was found to be 575°C. Also, based on the results in Table 10, the optimum pH for producing activated carbon with the best adsorptive performance using phosphoric acid from the tall tree variety

is 2.07 while that of the dwarf variety was found to be 1.98 of the acid solution. Based on the statistical analyses, the model's confidence interval between 95 and 99% gives correlation coefficient values with levels of accuracy in the range of 96–99%; hence, the model results agree well with data generated experimentally.

Nomenclature

Letters

C: Dye concentration after adsorption, [gL^{-1}]
N: Number of experiments, (—)
n: Number of factors, (—)
Y: Yield, [%]

Greek Symbols

ΔX_1: Change in concentration, [gL^{-1}]
ΔX_2: Change in temperature, [°C]
ΔY: Change in yield, [%].

TABLE 10: pH of the solutions (activating agents).

$ZnCl_2$, 1 M 29°C	KOH, 1 M 29°C	(0.3 M H_3PO_4) 29°C	(0.5 M H_3PO_4) 29°C	(0.67 M H_3PO_4) 29°C	(1.00 M H_3PO_4) 29°C	1.33 M (H_3PO_4) 29°C
5.26	11.18	2.20	2.17	2.07	1.98	1.96

TABLE 11: Statistical analysis of model.

Item measured	Optimization (dwarf) Figure 4(b)(i)	Optimization (tall) Figure 4(b)(ii)	Optimization (dwarf) Figure 4(c)(i)	Optimization (tall) Figure 4(c)(ii)
Standard error	2.735	6.796	14.334	5.7687
95% confidence interval	8.704	21.625	45.611	18.356
99% confidence interval	15.98	39.696	83.725	33.695
Standard deviation	5.471	13.592	28.668	11.537
Coefficient of variation	0.371	0.5146	0.5148	0.371
Correlation with experiment	0.994	0.9559	0.9559	0.9936

TABLE 12: Statistical analysis of model.

Item measured	Optimization (tall) Figure 6(b)(i)	Optimization (dwarf) Figure 6(b)(ii)	Optimization (tall) Figure 6(c)(i)	Optimization (dwarf) Figure 6(c)(ii)
Standard error	6.796	2.7353	5.769	14.334
95% confidence interval	21.625	8.7037	18.36	45.611
99% confidence interval	39.696	15.977	33.69	83.725
Standard deviation	13.592	5.4706	11.54	28.668
Coefficient of variation	0.5146	0.3708	0.371	0.5148
Correlation with experiment	0.9559	0.9936	0.994	0.9559

Sub- and Superscripts

A_1: Tall tree variety sample with 0.3 M phosphoric acid concentration

$A_{1.5}$: Tall tree variety sample with 0.5 M phosphoric acid concentration

A_2: Tall tree variety sample with 0.67 M phosphoric acid concentration

A_3: Tall tree variety sample with 1 M phosphoric acid concentration

A_4: Tall tree variety sample with 1.33 M phosphoric acid concentration

A_{1*}: Dwarf tree variety sample with 0.3 M phosphoric acid concentration

A_{2*}: Dwarf tree variety sample with 0.67 M phosphoric acid concentration

A_{3*}: Dwarf tree variety sample with 1 M phosphoric acid concentration

A_{4*}: Dwarf tree variety sample with 1.33 M phosphoric acid concentration

B_1: Tall tree sample with 0.67 M phosphoric acid carbonized at 450°C

B_2: Tall tree sample with 0.67 M phosphoric acid carbonized at 575°C

B_3: Tall tree sample with 0.67 M phosphoric acid carbonized at 700°C

B_4: Tall tree sample with 0.67 M phosphoric acid carbonized at 850°C

b_0: Constant (global mean), (—)

b_1: Coefficient, (—)

b_2: Coefficient, (—)

b_3: Coefficient, (—)

b_4: Coefficient, (—)

b_5: Coefficient, (—)

b_6: Coefficient, (—)

b_7: Coefficient, (—)

C_0: Initial dye concentration, [gL^{-1}]

m_1: Mass of container with lid plus original sample, [g]

m_2: Mass of container with lid plus dried sample, [g]

m_3: Mass of container with lid, [g]

m_4: Mass of empty crucible, [g]

m_5: Mass of crucible plus original sample, [g]

m_6: Mass of crucible plus ash, [g]

m_7: Mass in g of the crucible, lid, and sample before heating, [g]

m_8: Mass in g of the crucible, lid, and content after heating, [g]

m_c: Percentage by mass of moisture in the sample, [%]

n_c: Number of center runs, (—)
S_1: Sample activated with $ZnCl_2$, (—)
S_2: Sample activated with H_3PO_4, (—)
S_3: Sample activated with KOH, (—)
S_4: Tall tree variety sample without any activating agent
X_1: Concentration term, $[gL^{-1}]$
X_2: Temperature term, $[°C]$
dY/dX_1: Change in yield with concentration, $[Lg^{-1}]$
dY/dX_2: Change in yield with temperature, $[°C^{-1}]$.

Abbreviations

NAC: Nonactivated carbon
CAC: Commercial activated carbon.

Conflicts of Interest

The authors declare that they have no conflicts of interest.

Acknowledgments

References

[1] A. A. Awoyale, A. C. Eloka-Eboka, and O. A. Odubiyi, "Production and experimental efficiency of activated carbon from local waste bamboo for waste water treatment," *International Journal of Engineering and Applied Sciences*, vol. 3, no. 2, pp. 1–10, 2013.

[2] M. A. Baghapour, B. Djahed, and M. Ranjbar, "Removal of methylene blue from aqueous solutions by waste paper derived activated carbon," *Journal of Health Science Surveillance Systems*, vol. 1, no. 1, pp. 48–56, 2013.

[3] R. C. Basal, *Activated Carbon Adsorption*, Dekker/CRC Press, Boca Raton, FL, USA, 1937.

[4] C. Gimba, *[Ph.D. thesis]*, Ahmadu Bello University, Zaria, Nigeria, 2001.

[5] M. K. B. Gratuito, T. Panyathanmaporn, R. A. Chumnanklang, and A. Dutta, "Production of activated carbon from coconut shell: optimization using response surface methodology," *Bioresource Technology*, vol. 99, no. 11, pp. 4887–4895, 2008.

[6] R. H. Gumus and I. Okpeku, "Production of activated carbon and characterization from snail shell waste (helix pomatia)," *Advances in Chemical Engineering and Science*, vol. 5, pp. 51–61, 2015.

[7] R. H. Hesas, A. Arami-Niya, W. M. A. Daud, and J. N. Sahu, "Preparation and characterization of activated carbon from apple waste by micro-assisted phosphoric acid activation: application in methylene blue adsorption," *Bioresources.com*, pp. 1–17, 2013.

[8] J. J. Hung, [B.Eng. thesis], Department of Chemical Engineering, University of Arizona, USA, 2012.

[9] A. W. M. Ip, J. P. Barford, and G. Mckay, "Production and comparison of high surface area bamboo derived active carbons," *Bioresource Technology*, vol. 6, pp. 6809–6816, 2008.

[10] H. Jankowska, A. Swiatkowski, and J. E. H. Choma, *Active Carbon*, West Sussex, England and Prentice-Hall, Englewood Cliffs, New Jersey, NJ, USA, 1991.

[11] F. Karacan, U. Ozden, and S. Karacan, "Optimization of manufacturing conditions for activated carbon from Turkish lignite by chemical activation using response surface methodology," *Applied Thermal Engineering*, vol. 27, no. 7, pp. 1212–1218, 2007.

[12] J. M. Ketcha, D. J. M. Dina, H. M. Ngomo, and N. J. Ndi, "Preparation and characterization of activated carbons obtained from maize cobs by zinc chloride activation," *American Chemical Science Journal*, vol. 4, pp. 136–160, 2012.

[13] X. Long, H. Chang, and W. Yuan, "Reduction of hexamine cobalt (III) catalyzed by coconut activated carbon," *Environment Bryer and Sustainable Energy*, vol. 29, no. 1, pp. 85–92, 2010.

[14] P. A. M. Mourão, C. Laginhas, F. Custódio, J. M. V. Nabais, P. J. M. Carrott, and M. M. L. R. Carrott, "Influence of oxidation process on the adsorption capacity of activated carbons from lignocellulosic precursors," *Fuel Processing Technology*, vol. 92, no. 2, pp. 241–246, 2011.

[15] O. E. Odebunmi and O. F. Okeola, "Preparation and characterization of activated carbon from waste material," *Journal of Chemical Society of Nigeria*, vol. 26, no. 2, pp. 1–7, 2001.

[16] N. H. Phan, S. Rio, C. Faur, L. Le Coq, P. Le Cloirec, and T. H. Nguyen, "Production of fibrous activated carbons from natural cellulose (jute, coconut) fibers for water treatment applications," *Carbon*, vol. 44, no. 12, pp. 2569–2577, 2006.

[17] F. Rodriguez-Reinoso, M. Molina-Sabio, and M. Gonzalez, "The use of steam and CO as activating agents in the preparation of activated carbons," *Carbon*, vol. 33, no. 1, pp. 15–23, 1995.

[18] J. Romanos, M. Beckner, T. Rash et al., "Nanospace engineering of KOH activated carbon," *Nanotechnology*, vol. 23, no. 1, pp. 15401–15407, 2012.

[19] U. Sains and N. Sembilan, "Preparation and characterization of activated carbon from desiccated coconut residue by potassium hydroxide," *Asian Journal of Chemistry*, vol. 27, no. 6, pp. 2331–2336, 2015.

[20] T. Shalna and A. Yogamoorthi, "Preparation and characterization of activated carbon from used tea dust in comparison with commercial activated carbon," *International Journal of Recent Scientific Research*, vol. 6, no. 2, pp. 2750–2755.

[21] O. A. Sodeinde, "Preparation of a locally produced activated carbon from coconut shells and its use in reducing hexamine cobalt III," *International Journal of Chemical Engineering and Applications*, vol. 3, no. 1, pp. 1–5.

[22] M. Soleimani and T. Kagazchi, "Low-Cost adsorbents from agricultural by-products impregnated with phosphoric acid," *Advanced Chemical Engineering Research*, vol. 3, pp. 1–8, 2014.

[23] P. Susheela and R. Radha, "Production of activated carbon from dry coconut shell and its efficacy in treating waste water," *International Journal of Chemical and Biological Sciences*, vol. 1, no. 10, pp. 1–9.

[24] C. Srinivasakannan and M. Abu Bakar, "Production of activated carbon from rubber wood sawdust," *Biomass and Bioenergy*, vol. 27, no. 1, pp. 89–96, 2004.

[25] N. A. Taha, S. E. Abdelhafez, and A. El-Maghraby, "Chemical and physical preparation of activated carbon using raw bagasse pith for cationic dye adsorption," *Global Nest Journal*, vol. 18, no. 2, pp. 1–14, 2016.

[26] I. A. W. Tan, A. L. Ahmad, and B. H. Hameed, "Preparation of activated carbon from coconut husk: optimization study on removal of 2,4,6-trichlorophenol using response surface methodology," *Journal of Hazardous Materials*, vol. 153, no. 1-2, pp. 709–717, 2008.